J Sol-Gel Sci Technol (2017) 81:42–51
DOI 10.1007/s10971-016-4077-1

ORIGINAL PAPER: NANO- AND MACROPOROUS MATERIALS (AEROGELS, XEROGELS, CRYOGELS, ETC.)

Low-density, transparent aerogels and xerogels based on hexylene-bridged polysilsesquioxane with bendability

Yosuke Aoki[1] · Taiyo Shimizu[1] · Kazuyoshi Kanamori[1] · Ayaka Maeno[2] · Hironori Kaji[2] · Kazuki Nakanishi[1]

Received: 5 January 2016 / Accepted: 17 May 2016 / Published online: 24 May 2016

Abstract Low-density, transparent aerogels based on a hexylene-bridged polysilsesquioxane ($[O_{1.5}Si–(CH_2)_6–SiO_{1.5}]_n$) network have been prepared for the first time via a simple sol–gel process. An optimized base-catalyzed one-step hydrolysis–polycondensation process of a bridged alkoxysilane precursor 1,6-bis(trimethoxysilyl)hexane in a low-polarity solvent *N*,*N*-dimethylformamide allows for the formation of a pore structure of a length scale of several tens nanometers, resulting in low-density, transparent aerogels after supercritical drying. Because of the incorporated organic moiety that bridges the silicon atoms in the network, these aerogels show higher flexibility and strength against compression and bending as compared to silica aerogel counterparts. In addition, minimizing the residual silanol groups in the network by a surface modification with hexamethyldisilazane has further improved resilience after compression and bending flexibility and strength, due to the decreased chance of the irreversible formation of the siloxane bonds upon compression. The resulting trimethylsilylated hydrophobic gels have been subjected to ambient pressure drying to obtain xerogels, resulting in low-density (0.13 g cm^{-3}, 90 % porosity), transparent (71 % transmittance) xerogels. These results are promising for the development of transparent thermal superinsulators applicable to window insulating systems that manage heat transfer in a more efficient way.

Graphical Abstract

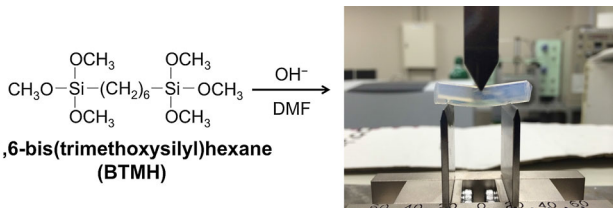

Keywords Bridged polysilsesquioxane · Hexylene · Aerogels · Xerogels · Optical and mechanical properties

1 Introduction

Aerogels are regarded as a unique class of solid materials differentiated by low density and high porosity [1–4]. The typical aerogels based on silica have been studied for more than 80 years since the first invention by Kistler [5], and research on their preparation and control over physical properties is well established [6]. The pursuit of aerogel materials is still developing, because carefully prepared aerogels show extremely low thermal conductivity as a solid material and would contribute to the reduction of energy consumption if applied as thermal superinsulators in many aspects in domestic and industrial uses [7, 8]. For this purpose, however, the following two critical issues in silica aerogels must be overcome: the low mechanical properties and the necessity of supercritical drying. The low mechanical properties such as friability against compression and bending make the handling of aerogels difficult and discourage the formability, and demining of this issue in fact can lead to a development of easier drying

✉ Kazuyoshi Kanamori
kanamori@kuchem.kyoto-u.ac.jp

[1] Department of Chemistry, Graduate School of Science, Kyoto University, Kitashirakawa, Sakyo-ku, Kyoto 606-8502, Japan

[2] Division of Environmental Chemistry, Institute for Chemical Research, Kyoto University, Gokasho, Uji 611-0011, Japan

process that does not rely on supercritical fluid at high pressure (and temperature). A lot of research activities have been devoted to improve the mechanical properties [9] by organic–inorganic hybridization involving the use of organo-substituted silane precursors [10–13] and cross-linking the surface of functionalized silica backbone with organic polymers such as epoxides [14], isocyanates [15] and styrene [16]. Besides successful mechanical improvements, both strategies have encountered several drawbacks, the major ones of which are enlargement of the pores and increase in bulk density. The former is typical in the preparation of aerogels from organo-substituted alkoxysilanes, since the formation of hydrophobic networks induces macroscopic phase separation to give pores typically in the micrometer range [17, 18]. The latter is resulted from guest molecules cross-linked on the pore surface. Visible light transparency of aerogels is a key factor when considering applications to thermal superinsulators due to the following reason; transparency is the result of sufficiently fine pore and skeleton structures with high homogeneity [19, 20], and optimized superinsulating ability can be achieved when the solid- and gas-phase thermal conduction is minimized at adequately low bulk density ($\sim$0.15 g cm^{-3}) and with pore size shorter than the mean free path of molecules in air (ca. 68 nm for nitrogen at 10^5 Pa 300 K) [21]. In other words, when the solid skeleton does not have strong visible light absorption, transparency can be a useful guide to envisage the low thermal conductivity. It is also worth noting that preparation of superinsulating aerogel via conventional evaporative drying at ambient conditions had been fairly limited [22] except for granules and powders [23, 24].

We have been studying organic–inorganic hybrid aerogels from organo-substituted alkoxysilane precursors to improve mechanical properties under the concept that the main origin of the low mechanical properties can be attributed to the rigid (not flexible) tetrafunctional polysiloxane networks in silica gel and to the resultant friability in the neck part of the solid skeletons of weakly connected colloids [25]. Replacing tetraalkoxysilanes in the sol–gel preparation of silica aerogels with alkyltrialkoxysilanes is found to give rise to the appreciable improvement in the mechanical properties. Through synthetic improvements, we have obtained low-density, transparent aerogels based on polymethylsilsesquioxane (PMSQ, mainly composed of a $CH_3SiO_{1.5}$ random network) for the first time from methyltrimethoxysilane (MTMS) via a two-step acid–base sol–gel process under the presence of a surfactant, and a perfect shrinkage–reexpansion (spring-back) behavior has been observed on uniaxial compression–decompression [26–29]. The optimized PMSQ aerogel undergoes 80 % linear compression without cracking or collapsing and recovers original size and shape after unloaded. This extraordinary behavior also allows for a successful preparation of aerogel-like xerogels through evaporative drying under ambient pressure and temperature. The preparation of low-density, transparent, superinsulating PMSQ xerogels has already been established, and large-area xerogel tiles (such as 250 $\times$ 250 $\times$ 10 mm^3) can be produced with good reproducibility [30].

Another interesting precursor for flexible aerogels is bridged alkoxysilanes [$(R'O)_3Si–R–Si–(OR')_3$, where R is typically alkyl or aryl]. The sol–gel research of these precursors was originated by Shea and Loy [31, 32], and the bridged polysilsesquioxane network ($[O_{1.5}Si-R-SiO_{1.5}]_n$) with surfactant-templated periodic mesopores is known as periodic mesoporous organosilicas (PMOs) [33–35]. Bridged polysilsesquioxane aerogels from these precursors have also been a research target because these hexafunctional precursors can form monolithic gels even at low concentrations like 0.1 M [36], which is advantageous in preparing low-density solids. Among typical alkoxysilanes bridged with alkylene, arylene, and other groups, one with a relatively long and flexible bridging group, 1,6-bis(trialkoxysilyl)hexane, is an attractive candidate to impart flexibility to the polysiloxane-based network. Loy et al. [37, 38] already reported preparations of hexylene-bridged polysilsesquioxane aerogels with high degree of condensation and low bulk density of <0.1 g cm^{-3}, though aerogels with transparency and improved flexural strength compared to silica aerogel counterparts have not been reported. A vapor-phase chemical modification of resultant aerogels with polycyanoacrylate effectively increased the flexural strength [39], and compressive modulus and strength were also reported to be improved by a chemical modification with hexamethyldisilazane (HMDS) or hexachlorodisilane [40]. Other groups demonstrated preparation and mechanical properties of bridged polysilsesquioxane porous gels with larger pore sizes typically in the micrometer range [41–43]. These opaque gels are highly flexible and can be used for separation of oil and water by soaking/squeezing with hand.

In the present study, aiming at potential applications to transparent thermal superinsulators, transparent aerogels based on hexylene-bridged polysilsesquioxane have been successfully prepared for the first time, and their mechanical properties have been investigated by uniaxial compression and three-point bending. Differences from silica aerogel counterparts is discussed to clarify the role of hexylene bridges in the polysiloxane network.

2 Experimental

2.1 Reagents

N,N-Dimethylformamide (DMF, special grade) trifluoroacetic acid (TFA, special grade), 1,1,1,3,3,3-hex-

amethyldisilazane (HMDS, special grade), 2-propanol (IPA, extra pure grade) and *n*-hexane (extra pure grade) were purchased from Kishida Chemical Ltd. (Japan). Distilled water (special grade) was from Hayashi Pure Chemical Ltd. (Japan). The precursor 1,6-bis(trimethoxysilyl)hexane (BTMH) was from Gelest Inc. (USA). Tetramethylammonium hydroxide (TMAOH, 25 % in water) was from Tokyo Chemical Industry Co., Ltd. (Japan). All reagents were used as received.

2.2 Preparation of aerogels and xerogels (Scheme 1)

All the starting compositions investigated in this study are listed in Table 1, and the experimental procedures are given in Schemes 1 (no post-treatment) and 2 (post-treatment with HMDS). The range of molar ratio is BTMH/water/TMAOH = 1:(2.55–4.47):(0.0345–0.173). In a glass vial, 3.50 mL of DMF and a given amount of BTMH were mixed, and then, a given amount of aqueous TMAOH was added to the vial under vigorous stirring. After 2-min stirring at room temperature, the sol was transferred into a stainless steel container or a tetrafluoroethylene perfluoroalkoxy alkane (PFA) tube (cylindrical samples for the three-point bending test) for gelation. Gelation (typically 1 h) and aging for 2 d in an oven at 60 °C were followed by aging in water for 1 d in an oven at 60 °C. After aging, gels were washed and solvent-exchanged with IPA at 60 °C for five times. Finally, CO_2 supercritical drying at 80 °C and 14 MPa was conducted for 10 h to obtain dried aerogel samples. Some of the alcogels in IPA were solvent-exchanged with *n*-hexane in a similar way and slowly dried at ambient pressure at 40 °C for 3 d followed by 150 °C for 3 h to obtain xerogels.

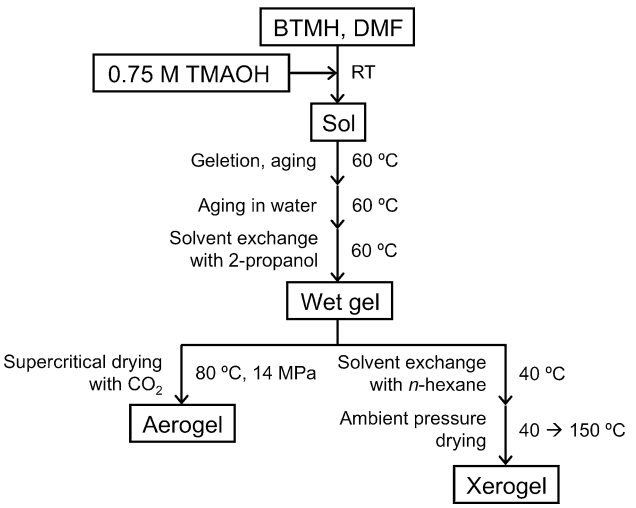

Scheme 1 Synthetic procedure for aerogels and xerogels without post-treatment

Sample names are given in the following format: BT$x-y$, where x and y denote hundred times the volumes (in mL) of BTMH and TMAOH aq., respectively. For example, BT40-15 means the one prepared from 0.40 mL of BTMH and 0.15 mL of 0.75 M TMAOH. Please note that the volume of DMF solvent is fixed as 3.50 mL in all cases unless otherwise mentioned.

2.3 Preparation of hydrophobic aerogels and xerogels (Scheme 2)

Hydrophobic aerogels were prepared via trimethylsilylation with HMDS. Wet gels washed with IPA were solvent-exchanged with *n*-hexane at 40 °C for three times. After solvent exchange in *n*-hexane, the gels were transferred into a mixture of HMDS, TFA and *n*-hexane to modify the surface of the wet gels. After trimethylsilylation for 3 d at 40 °C, the gels were washed with *n*-hexane two times in order to remove the unreacted trimethylsilylating agent. For evaporative drying at ambient pressure and temperature, the washed samples were put in an oven at 40 °C for 3 d followed by 150 °C for 3 h to obtain xerogels. For supercritical drying for comparison, the washed samples were solvent-exchanged with IPA at 60 °C for three times and undergo CO_2 supercritical drying at 80 °C and 14 MPa for 10 h, to obtain aerogels.

2.4 Measurements

The porous morphology of obtained aerogels was observed with a field emission scanning electron microscope (FE-SEM, JSM-6700F, JEOL, Japan). Bulk density was calculated from the weight/volume ratio of the aerogel samples. For near-infrared (NIR) spectroscopy and visible light transmittance measurements, a UV–Vis–NIR spectrometer V-670 (JASCO Corp., Japan) equipped with an integrating sphere ISN-732 was employed. Total light transmittance at 550 nm was normalized to the value of 10 mm thickness by the Lambert–Beer equation. The normalized visible light transmittance is denoted as T. ^{29}Si and ^{13}C solid-state NMR measurements were conducted on an Avance III 800 MHz (Bruker, Germany) spectrometer operating under a static magnetic field of 18.8 T. A double-resonance probe with a 4.0-mm magic angle spinning (MAS) probehead was used. For cross-polarization (CP) processes, optimized contact times were used: 5.5 and 4.0 ms for ^{29}Si and ^{13}C CP/MAS measurements, respectively. The ^{29}Si chemical shifts were expressed as values relative to tetramethylsilane (Me_4Si) by using the resonance line at −9.66 ppm for hexamethylcyclotrisiloxane crystals as an external reference. The ^{13}C chemical shifts were expressed as values relative to Me_4Si by using the carbonyl carbon resonance line at 176.46 ppm for glycine crystals as an external

Table 1 Starting compositions and obtained properties of aerogels[a]

	BTMH/mL	0.75 M TMAOH/mL	ρ_b^c/g cm^{-3}	ε^d/%	T^e/%
BT20-15	0.20	0.15	0.16	88	22
BT25-15	0.25	0.15	0.18	86	36
BT30-15	0.30	0.15	0.20	85	40
BT35-15	0.35	0.15	0.18	86	49
BT40-15	0.40	0.15	0.20	85	54
BT40-15H[b]	0.40	0.15	0.18	86	56
BT45-15	0.45	0.15	0.22	83	58
BT35-05	0.35	0.05	0.14	89	45
BT35-10	0.35	0.10	0.20	85	48
BT35-20	0.35	0.20	0.20	84	42
BT35-25	0.35	0.25	0.20	85	37
BT60-15	0.60	0.15	0.22	83	57
BT60-15H[b]	0.60	0.15	0.22	83	56

[a] The amount of DMF is fixed as 3.5 mL

[b] Treated with HMDS before drying

[c] Bulk density

[d] Porosity obtained by $(1 - \rho_b/\rho_s) \times 100$ with ρ_s being skeletal density of 1.29 g cm^{-3} [47]

[e] Light transmittance at 550 nm through 10 mm equivalent specimen

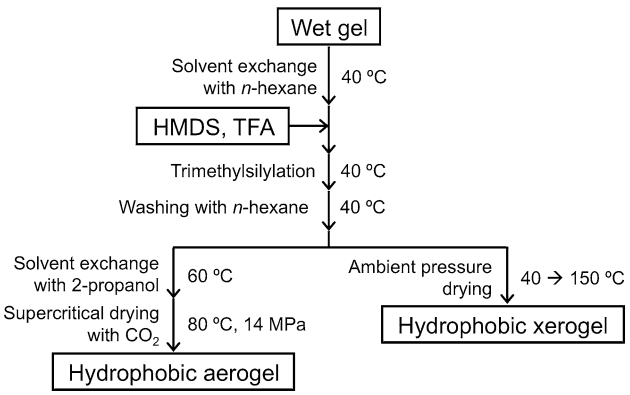

Scheme 2 Synthetic procedure for hydrophobic aerogels and xerogels with post-treatment with HMDS

reference. The MAS spinning speed was set to 15 kHz throughout this work. Mechanical properties of aerogels were investigated with a material tester EZGraph (Shimadzu Corp., Japan). For uniaxial compression, carved aerogels (typically bottom is ca. 10 × 10 mm^2 and height is ca. 6 mm) are compressed using a load cell of 5 kN. The measurements were performed in the strain of 0–50 % by uniaxial compression at a speed of 0.5 mm min^{-1} and then decompressed back to 0 N at the same speed. For three-point bending, cylindrical-shaped (typical diameter of cross section is ca. 7 mm) aerogels were bent using a load cell of 5 N with a distance between fulcrums of 20 mm. The measurements were performed at a speed of 0.5 mm min^{-1} until rupture occurs. Raman spectra were measured with a Raman microscope XploRa (HORIBA, Ltd., Japan) with an incident laser beam at 532 nm. Nitrogen adsorption–desorption measurements with BELSORP-max (MicrotracBEL Corp., Japan) were performed on selected samples to evaluate Brunauer–Emmett–Teller (BET) surface area. The samples were degassed under vacuum at 80 °C overnight prior to the measurement.

3 Results and discussion

3.1 Pore properties of obtained aerogels

Appearances of the obtained aerogels from starting solutions listed in Table 1 are shown in Fig. 1, and microscopic structures of some of the obtained aerogels are presented in Fig. 2. All these samples were prepared in the solvent DMF, and no transparent or translucent samples have been obtained in a number of other solvents including alcohols (such as methanol), cyclic ethers (such as 1,4-dioxane and tetrahydrofuran), dimethylsulfoxide, acetone and *N*-methylformamide. Only DMF and *N*,*N*-dimethylacetamide (DMAc) gave transparent or translucent aerogels. Those prepared in DMAc were less transparent compared to those prepared in DMF. The microstructures obtained with DMF are the finest and most homogeneous compared to those obtained with other solvents. In addition to the specific hydrogen bonding between amides and silanol groups [44, 45], which is the basis for homogeneously incorporating organic polymers in the sol–gel-derived silica gel matrix, it

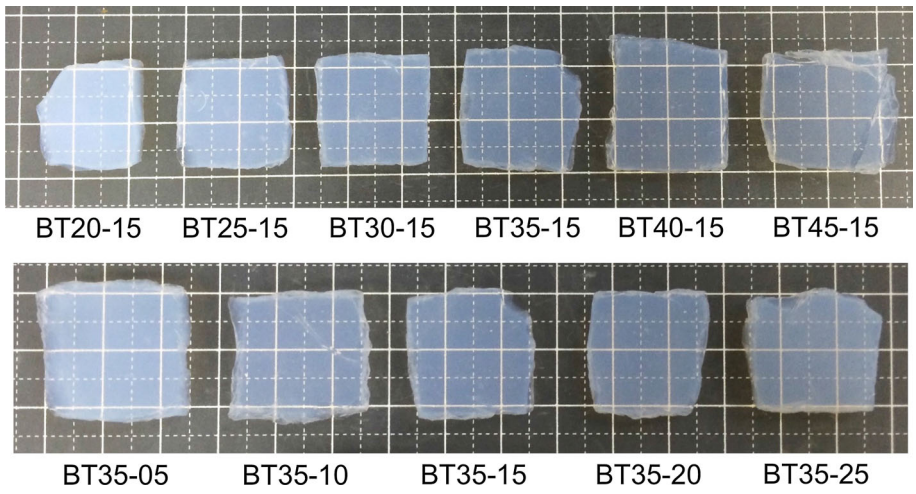

Fig. 1 Photographs of the hexylene-bridged polysilsesquioxane aerogels obtained in the present study. See Table 1 for starting composition

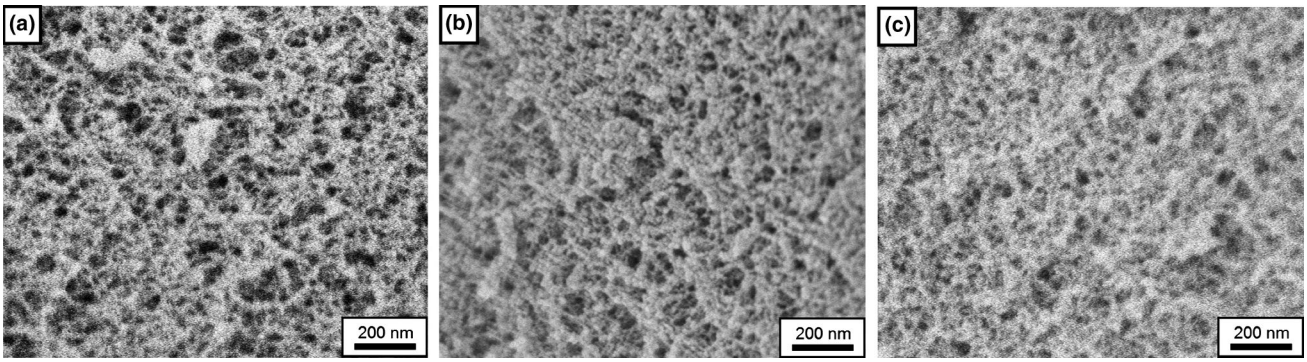

Fig. 2 FE-SEM images of aerogels; **a** BT25-15, **b** BT35-15, **c** BT45-15

should be noted that the difference in polarity (solubility parameter) of the polysilsesquioxane network and solvent has to be minimized to avoid phase separation in the course of sol–gel transition, because the phase separation induces submicron- to micrometer-scaled coarsened structures that scatter visible light [46].

Figure 3 exhibits the relationship among transparency, bulk density and the amount of BTMH/0.75 M TMAOH aq. in the starting solution. In part (a) showing BT*x*-15 series, bulk density naturally increases with increasing amount of BTMH, which can be also correlated with the microstructure by FE-SEM; structure becomes denser with increasing BTMH. In addition, light transmittance at 550 nm through 10 mm equivalent thickness also increases with increasing BTMH, because the porous structure becomes finer. The highest light transmittance reaches 58 % at bulk density of 0.22 g cm^{-3}. With increasing amount of TMAOH in BT35-*x* series shown in part (b), bulk density shows nearly constant values irrespective of the amount of TMAOH aq. Bulk density of BT35-05 is somewhat lower presumably due to incomplete hydrolysis and polycondensation of BTMH with the limited amount of water ($[H_2O]/[BTMH] = 2.55$). Transmittance decreases with increasing TMAOH aq., since the phase separation is enhanced. The concentration and kind of base (TMAOH and NaOH) did not give considerable effects in the aerogel properties in the range between 0.5 and 1 M, but cracks more easily developed in the samples prepared with NaOH as base. The increasing amount of solvent DMF (2.50–4.50 mL, with BTMH 0.35 mL and 0.75 M TMAOH 0.15 mL) reduces transmittance from 63 to 44 % with a decrease of bulk density from 0.25 to 0.21 g cm^{-3}.

Figure 4 presents ^{13}C and ^{29}Si solid-state CP/MAS NMR spectra of the aerogel sample BT40-15. Resonance peaks at 13.1, 23.5 and 33.0 ppm in the ^{13}C spectrum correspond to α β and γ carbons in the hexylene bridging unit [48]. The small peak at 50.2 ppm shows residual methoxy groups. In the ^{29}Si spectrum, peaks at −47.4, −56.7 and −66.3 ppm show, respectively, T^1, T^2 and T^3 unit of silicon, where T^n denotes the silicon species connected to the next silicon with n siloxane bonds. From these spectra, it is confirmed that highly cross-linked polysiloxane networks with preserved hexylene bridges has been formed. However, residual silanol groups attached to T^1 and T^2 species cause irreversible shrinkage by forming

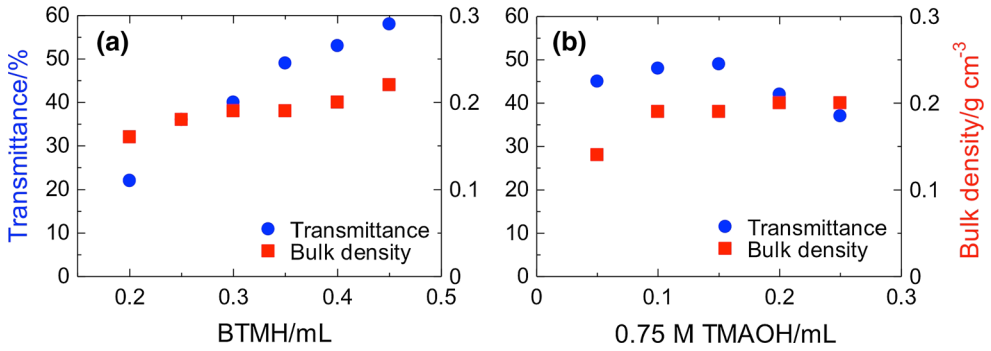

Fig. 3 Bulk density and visible light transmittance for aerogels prepared from different amounts of **a** BTMH and **b** TMAOH aq

new siloxane bonds [49] upon compression as described below.

3.2 Trimethylsilylation and its effects on the mechanical properties

Upon molecular-level structural analyses by NMR and NIR and mechanical tests as discussed below, it was found that a certain amount of silanol groups remains on the resultant aerogels, though the amount is smaller than those in acid-catalyzed gels [48]. Since uniaxial compression–decompression measurements show that aerogels are compressible without breaking but do not recover as discussed later, the silanols must be reduced for an improved spring-back behavior. We selected a standard silylating agent HMDS to reduce the silanols and render the silica-based gels hydrophobic [50, 51]. In Fig. 5, near-infrared (NIR) spectra of the non-treated BT40-15 and HMDS-treated BT40-15H samples show clear differences in the silanol absorption bands at ca. 4530 and 7250 cm^{-1} (combination of stretching and bending and first overtone of stretching of the vicinal silanols, respectively) [52]. In addition, the absorption band at 5283 cm^{-1}, assigned to the stretching–bending combination of hydrogen-bonded water, is disappeared after the treatment with HMDS. Further, the NMR spectra of BT40-15H shown in Fig. 4 present the appearance of trimethylsilyl groups by the new peaks at 0.1 ppm in ^{13}C (methyl carbon) and 7.7 ppm in ^{29}Si (M^1 silicon), accompanied by the decrease of T^1 and T^2 species. Thus, it can be concluded that the residual silanol groups are effectively reduced by the HMDS treatment. This successful surface modification changes the surface property of the treated aerogel into hydrophobic, and water forms droplet on the outer surface of the aerogel.

Mechanical compression–decompression behaviors of the non-treated, HMDS-treated and hydrophilic silica

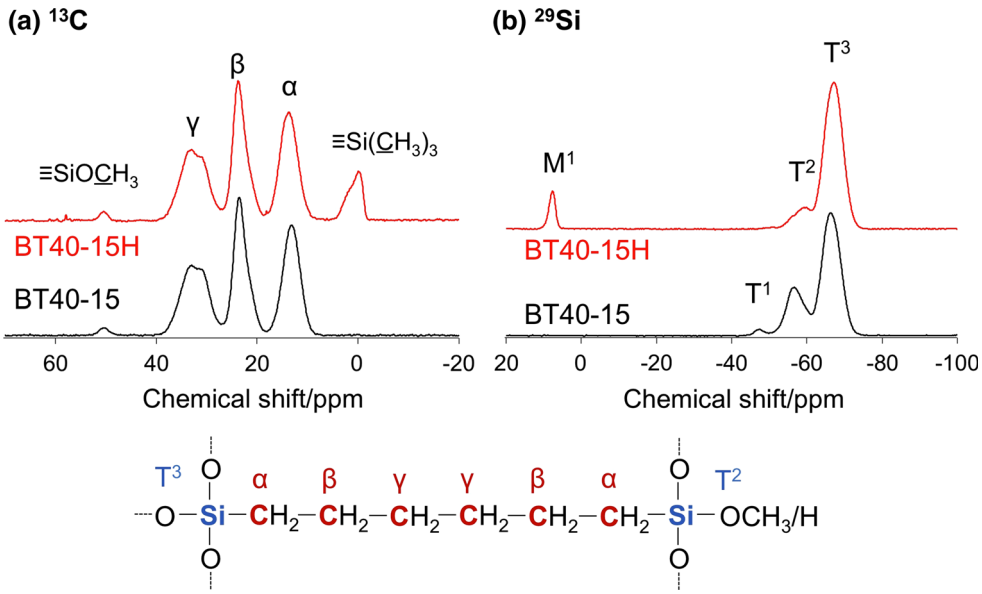

Fig. 4 **a** ^{13}C and **b** ^{29}Si CP/MAS NMR spectra of the sample without (BT40-15) and with (BT40-15H) silylation with HDMS

aerogel samples are compared in Fig. 6. Bulk density of the non-treated and treated samples (BT40-15 and BT40-15H, Table 1) is 0.20 and 0.18 g cm^{-3}, respectively. The non-treated hexylene-bridged silsesquioxane sample shows good strength and flexibility without breaking up to 50 % strain. In contrast, a silica aerogel with similar bulk density (0.20 g cm^{-3}) undergoes serious cracking and collapsing at strain as low as ca. 20 %. This striking difference results from differences in the network structure, in which every silicon in the polysiloxane network is bridged with the flexible hexylene unit in the polysilsesquioxane samples, and the hexylene bridges can deform to avoid the stress concentration in the material. Furthermore, the compression–decompression behavior of the HMDS-treated sample is further improved, meaning that resilience of the treated sample is lower (27 %) than that of the non-treated sample (40 %). The resilience of the treated sample can be further lowered to <10 % after the decompressed sample is heated at 80 °C for 1 d, because of enhanced relaxation of the contracted network and pore structures. The timescale of this relaxation behavior is more sluggish compared to the PMSQ counterparts, which show faster spring-back at the similar bulk density, presumably due to the enhanced viscoelasticity by the hexylene bridges. The similar behavior is also observed in organic polymer gels in which the time dependence of relaxation behavior varies depending on the cross-linking density, extent of chain entanglement and chemical structure [53–55].

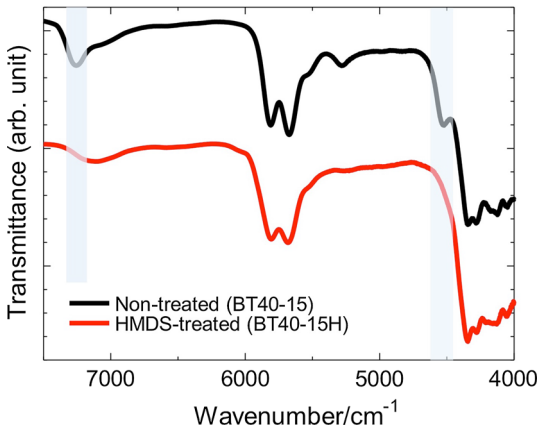

Fig. 5 Near-infrared spectra of the samples without (BT40-15) and with (BT40-15H) silylation by HMDS

Three-point bending tests have been performed on BT60-15 and BT-60-15H (bulk density of both is 0.22 g cm^{-3}), and the results are shown in Fig. 7 with that of silica aerogel at 0.20 g cm^{-3}. The bending property also demonstrates superior flexibility as compared to the silica counterpart due to the introduction of hexylene bridges in the polysiloxane network. The strain value at catastrophic collapse for BT60-15 is more than double compared to the silica counterpart, and bending strength at the collapse is also double. The HMDS-treated sample BT60-15H exhibits further improved bending flexibility and strength as is also shown in Fig. 8, due to the monolayer of the trimethylsilyl groups and their repulsive nature [40]. The maximum strain at failure is also around 40 % in the case of PMSQ aerogels with bulk density of 0.14 g cm^{-3} (not shown), and the hexylene-bridged polysilsesquioxane aerogels possess attractive potential to be a more flexible aerogel.

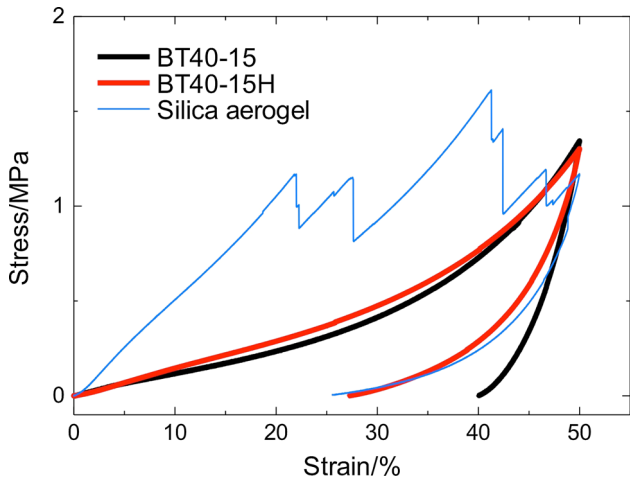

Fig. 6 Stress–strain curves obtained by uniaxial compression–decompression of aerogels without treatment (BT40-15, 0.20 g cm^{-3}) and with HMDS treatment (BT40-15H, 0.18 g cm^{-3}). For comparison, the stress–strain curve of silica aerogel (base-catalyzed, hydrophilic) with similar bulk density (0.20 g cm^{-3}) is also shown

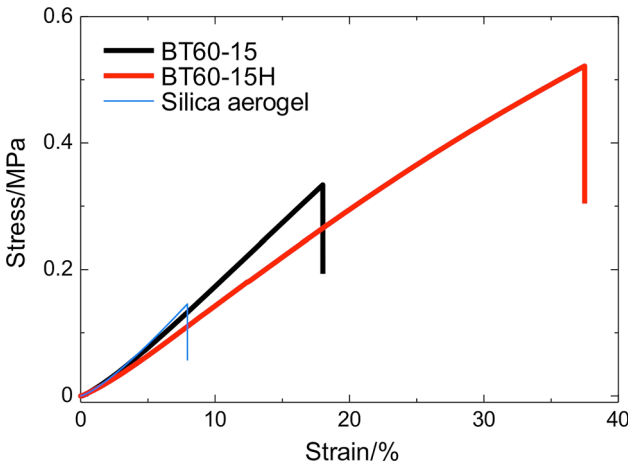

Fig. 7 Stress–strain curves obtained by three-point bending of aerogels without treatment (BT60-15, 0.22 g cm^{-3}) and with HMDS treatment (BT60-15H, 0.22 g cm^{-3}). For comparison, stress–strain curve of base-catalyzed hydrophilic silica aerogel with similar bulk density (0.20 g cm^{-3}) is also shown

3.3 Ambient pressure drying toward aerogel-like xerogels

Since the spring-back behavior on compression directly influences the same behavior in the course of evaporative drying, where the samples undergo a similar compression–decompression deformation cycle due to surface tension of the evaporating solvent, the reduced resilience is advantageous in the preparation of aerogel-like xerogels by ambient pressure drying, which is the most promising process to reduce the production cost [22, 56, 57]. During ambient pressure drying of the sample BT40-15(H), the temporal shrinkage and relaxing (spring-back) behavior have been observed in the course of evaporation of the solvent (and successive rigorous drying at 150 °C in the case of the HMDS-treated sample). Bulk density of BT40-15 xerogel is 0.31 g cm^{-3} and that of BT40-15H is 0.13 g cm^{-3}, which can be compared to those of supercritically dried aerogels (0.20 and 0.18 g cm^{-3}, respectively, Fig. 9; Table 2). Boday et al. [38] dried hexylene-bridged polysilsesquioxane hydrogels at an ambient condition, resulting in higher irreversible shrinkage and higher density (0.78 g cm^{-3}) due to the higher surface tension of the drying solvent, water. It is also reported that silica xerogel granules [58] and films consisting of homogenized particles [59] can be obtained from hydrophobized silica wet gels by ambient pressure drying accompanied by spring-back. However, no monolithic aerogel-like xerogels have been reported due to serious cracking during the spring-back process.

Bulk density of BT40-15H xerogel is largely lowered compared to the corresponding aerogel, though that of BT40-15 xerogel is apparently high due to irreversible shrinkage caused by residual silanols as mentioned earlier.

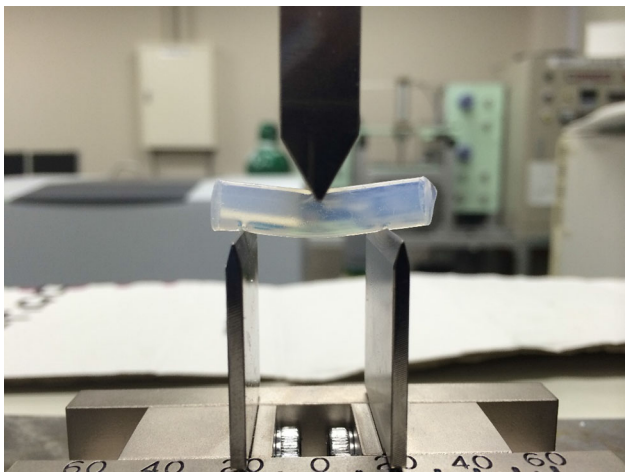

Fig. 8 Photograph showing the bendability of an HMDS-treated sample (BT60-15H) during three-point bending test

The network and porous structure in BT40-15H xerogel have been almost fully relaxed presumably because of the final drying at 150 °C for 3 h, whereas those in BT40-15H aerogel dried at 80 °C have not been fully relaxed from possible deformations of the viscoelastic network induced during the sol–gel and supercritical drying processes [60]. In addition, possibility of slight shrinkage during supercritical drying may come from finite contraction by non-ideal surface tension. The similar values of BET specific surface area of these samples suggest that there are negligible changes in the colloidal network structures even when there is serious shrinkage.

Light transmittance values of these samples are 68 % for BT40-15 and 71 % for BT40-15H (Table 2). Whereas BT40-15 xerogel is highly shrunk and densified, BT40-15H

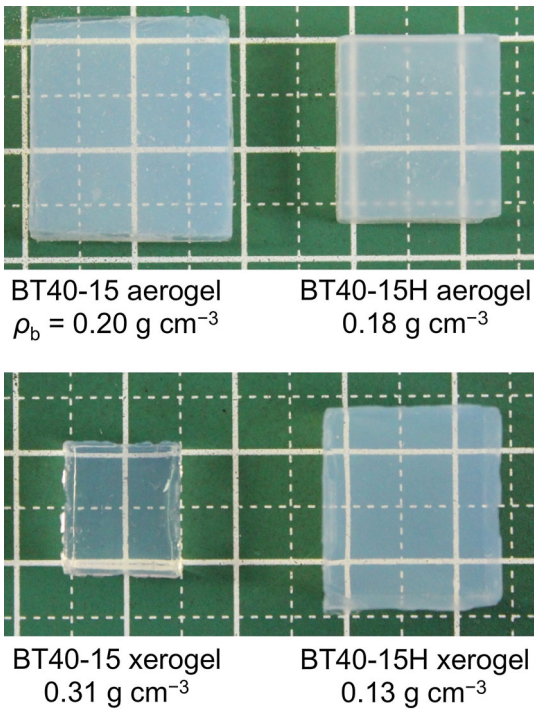

Fig. 9 Appearance of the aerogel from supercritical drying and xerogels from ambient pressure drying based on the starting composition BT40-15. Sample size does not accurately reflect irreversible shrinkage. Sample thickness of BT40-15H xerogel is 8 mm and the others 5 mm

Table 2 Starting compositions and obtained properties of aerogels

	ρ_b/g cm^{-3}	ε/%	T/%	a^a_{BET}/m^2 g^{-1}
BT40-15 aerogel	0.20	84	54	874
BT40-15H aerogel	0.18	86	56	924
BT40-15 xerogel	0.31	76	68	918
BT40-15H xerogel	0.13	90	71	893

[a] BET-specific surface area from nitrogen adsorption–desorption measurements

xerogel shows low density together with good light transmittance, which can be compared to standard silica aerogels and PMSQ xerogels. The low-density, transparent xerogel by ambient pressure drying has been for the first time obtained from a bridged alkoxysilane precursor.

4 Conclusions

Transparent aerogels have for the first time been prepared from 1,6-bis(trimethoxysilyl)hexane via a one-step base-catalyzed sol–gel process in a solvent *N*,*N*-dimethylformamide and supercritical drying. As compared to silica aerogel counterparts, the resulting hexylene-bridged polysilsesquioxane aerogels show improved bendability and compressibility without collapsing; however, they show limited resilience after unloaded. Since residual silanol groups in the resulting aerogels are found to hinder the shrinkage–reexpansion (spring-back) behavior on compression–decompression, a liquid-phase post-treatment with hexamethyldisilazane has been performed to minimize the silanol groups. This hydrophobization process leads to further improvements in the compression and bending properties in such a way as an improved spring-back behavior with higher resilience, which is advantageous in ambient pressure drying to obtain an aerogel-like xerogel. Evaporative drying from *n*-hexane has resulted in a monolithic xerogel with good transparency (71 % at 550 nm through 10 mm) and low density (0.13 g cm^{-3}). The hexylene-bridged polysilsesquioxane xerogel materials with the good mechanical properties are attractive as a candidate for practical thermal superinsulators.

Acknowledgments The present study has been performed under financial supports from Grant-in-Aid for Scientific Research (No. 24550253 JSPS and MEXT Japan) and Advanced Low Carbon Technology Research and Development Program (ALCA, JST Japan).

References

1. Hüsing N, Schubert U (1998) Aerogels-airy materials: chemistry structure and properties. Angew Chem Int Ed 37:22–45
2. Pierre AC, Pajonk GM (2002) Chemistry of aerogels and their applications. Chem Rev 102:4243–4265
3. Du A, Zhou B, Zhang Z, Shen J (2013) A special material or a new state of matter: a review and reconsideration of the aerogel. Materials 6:941–968
4. Kanamori K (2013) Recent progress in aerogel science and technology. Adv Porous Mater 1:147–163
5. Kistler SS (1931) Coherent expanded aerogels and jellies. Nature 127:741
6. Soleimani Dorcheh A, Abbasi MH (2008) Silica aerogels; synthesis properties and characterization. J Mater Process Tech 199:10–26
7. Baetens R, Jelle BP, Gustavsen A (2011) Aerogel insulation for building applications: a state-of-the-art review. Energy Build 43:761–769
8. Koebel M, Rigacci A, Achard PJ (2012) Aerogel-based thermal superinsulation: an overview. J Sol–Gel Sci Technol 63:315–339
9. Randall JP, Meador MAB, Jana SC (2011) Tailoring mechanical properties of aerogels for aerospace applications. ACS Appl Mater Interfaces 3:613–626
10. Rao AV, Kulkarni MM, Amalnerkar DP, Seth T (2003) Superhydrophobic silica aerogels based on methyltrimethoxysilane precursor. J Non-Cryst Solids 330:187–195
11. Rao AV, Bhagat SD, Hirashima H, Pajonk GM (2006) Synthesis of flexible silica aerogels using methyltrimethoxysilane (MTMS) precursor. J Colloid Interface Sci 300:279–285
12. Martín L, Ossó JO, Ricart S, Roig A, Garcíad O, Sastred R (2008) Organo-modified silica aerogels and implications for material hydrophobicity and mechanical properties. J Mater Chem 18:207–213
13. Guo H, Nguyen BN, McCorkle LS, Shonkwiler B, Meador MAB (2009) Elastic low density aerogels derived from bis[3-(triethoxysilyl)propyl]disulfide tetramethylorthosilicate and vinyltrimethoxysilane via a two-step process. J Mater Chem 19:9054–9062
14. Meador MAB, Fabrizio EF, Ilhan F, Dass A, Zhang G, Vassilaras P, Johnston JC, Leventis N (2005) Cross-linking amine-modified silica aerogels with epoxies: mechanically strong lightweight porous materials. Chem Mater 17:1085–1098
15. Katti A, Shimpi N, Roy S, Lu H, Fabrizio EF, Dass A, Capadona LA, Leventis N (2006) Chemical physical and mechanical characterization of isocyanate cross-linked amine-modified silica aerogels. Chem Mater 18:285–296
16. Mulik S, Sotiriou-Leventis C, Churu G, Lu H, Leventis N (2008) Cross-linking 3D assemblies of nanoparticles into mechanically strong aerogels by surface-initiated free-radical polymerization. Chem Mater 20:5035–5046
17. Nakanishi K, Kanamori K (2005) Organic–inorganic hybrid poly(silsesquioxane) monoliths with controlled macro- and mesopores. J Mater Chem 15:3776–3786
18. Dong H, Brook MA, Brennan JD (2005) A new route to monolithic methylsilsesquioxanes: gelation behavior of methyltrimethoxysilane and morphology of resulting methylsilsesquioxanes under one-step and two-step processing. Chem Mater 17:2807–2816
19. Cao W, Hunt AJ (1994) Improving the visible transparency of silica aerogels. J Non Cryst Solids 176:18–25
20. Emmerling A, Petricevic R, Beck A, Wang P, Scheller H, Fricke J (1995) Relationship between optical transparency and nanostructural features of silica aerogels. J Non Cryst Solids 185:240–248
21. Lu X, Arduini-Schuster MC, Kuhn J, Nilsson O, Fricke J, Pekala RW (1992) Thermal conductivity of monolithic organic aerogels. Science 255:971–972
22. Aravind PR, Shajesh P, Soraru GD, Warrier KGK (2010) Ambient pressure drying: a successful approach for the preparation of silica and silica based mixed oxide aerogels. J Sol–Gel Sci Technol 54:105–117
23. Schwertfeger F, Schmidt DFM (1998) Hydrophobic waterglass based aerogels without solvent exchange or supercritical drying. J Non Cryst Solids 225:24–29
24. Land VD, Harris TM, Teeters DC (2001) Processing of low-density silica gel by critical point drying or ambient pressure drying. J Non Cryst Solids 283:11–17
25. Hæreid S, Anderson J, Einarsrud MA, Hua DW, Smith DM (1995) Thermal and temporal aging of TMOS-based aerogel precursors in water. J Non Cryst Solids 185:221–226

26. Kanamori K, Aizawa M, Nakanishi K, Hanada T (2007) New transparent methylsilsesquioxane aerogels and xerogels with improved mechanical properties. Adv Mater 19:1589–1593
27. Kanamori K, Nakanishi K, Hanada T (2009) Sol–gel synthesis porous structure and mechanical property of polymethylsilsesquioxane aerogels. J Ceram Soc Jpn 117:1333–1338
28. Hayase G, Kanamori K, Nakanishi K (2012) Structure and properties of polymethylsilsesquioxane aerogels synthesized with surfactant *n*-hexadecyltrimethylammonium chloride. Microporous Mesoporous Mater 158:247–252
29. Kurahashi M, Kanamori K, Takeda K, Kaji H, Nakanishi K (2012) Role of block copolymer surfactant on the pore formation in methylsilsesquioxane aerogel systems. RSC Adv 2:7166–7173
30. Kanamori K (2014) Monolithic silsesquioxane materials with well-defined pore structure. J Mater Res 29:2773–2786
31. Shea KJ, Loy DA (2001) Bridged polysilsesquioxanes. Molecular-engineered hybrid organic–inorganic materials. Chem Mater 13:3306–3319
32. Hu LC, Shea KJ (2011) Organo–silica hybrid functional nanomaterials: how do organic bridging groups and silsesquioxane moieties work hand-in-hand. Chem Soc Rev 40:688–695
33. Stein A, Melde BJ, Schroden RC (2000) Hybrid inorganic–organic mesoporous silicates—nanoscopic reactors coming of age. Adv Mater 19:1403–1419
34. Hatton B, Landskron K, Whitnall W, Perovic D, Ozin GA (2005) Past present and future of periodic mesoporous organosilicas-the PMOs. Acc Chem Res 38:305–312
35. Mizoshita N, Tani T, Inagaki S (2011) Syntheses, properties and applications of periodic mesoporous organosilicas prepared from bridged organosilane precursors. Chem Soc Rev 40:789–800
36. Baugher BM, Loy DA, Prabakar S, Assink RA, Shea KJ, Oviatt H (1995) Porosity in hexylene-bridged polysilsesquioxanes. Effects of monomer concentration. Mater Res Soc Symp Proc 371:253–259
37. Loy DA, Jamison GM, Baugher BM, Russick EM, Assink RA, Prabakar S, Shea KJ (1995) Alkylene-bridged polysilsesquioxane aerogels: highly porous hybrid organic–inorganic materials. J Non Cryst Solids 186:44–53
38. Boday DJ, Stover RJ, Muriithi B, Loy DA (2012) Mechanical properties of hexylene- and phenylene-bridged polysilsesquioxane aerogels and xerogels. J Sol–Gel Sci Technol 61:144–150
39. Boday DJ, Stover RJ, Muriithi B, Loy DA (2011) Strong low density hexylene- and phenylene-bridged polysilsesquioxane aerogel-polycyanoacrylate composites. J Mater Sci 46:6371–6377
40. Obrey KAD, Wilson KV, Loy DA (2011) Enhancing mechanical properties of silica aerogels. J Non Cryst Solids 357:3435–3441
41. Wang Z, Dai Z, Wu J, Zhao N, Xu J (2013) Vacuum-dried robust bridged silsesquioxane aerogels. Adv Mater 25:4494–4497
42. Yun S, Luo H, Gao Y (2015) Low-density hydrophobic highly flexible ambient-pressure-dried monolithic bridged silsesquioxane aerogels. J Mater Chem A 3:3390–3398
43. Wang Z, Wang D, Qian Z, Guo J, Dong H, Zhao N, Xu J (2015) Robust superhydrophobic bridged silsesquioxane aerogels with tunable performances and their applications. ACS Appl Mater Interfaces 7:2016–2024
44. Chujo Y, Saegusa T (1992) Organic polymer hybrids with silica gel formed by means of the sol–gel method. Adv Polym Sci 100:11–29
45. Ogoshi T, Chujo Y (2005) Organic–inorganic polymer hybrids prepared by the sol–gel method. Compos Interfaces 11:539–566
46. Nakanishi K (1997) Pore structure control of silica gels based on phase separation. J Porous Mater 4:67–112
47. Cerveau G, Corriu RJP, Framery E (2000) Sol–gel process: influence of the temperature on the textural properties of organosilsesquioxane materials. J Mater Chem 10:1617–1622
48. Loy DA, Obrey-DeFriend KA, Wilson KV Jr, Minke M, Baugher BM, Baugher CR, Schneider DA, Jamison GM, Shea KJ (2013) Influence of the alkoxide group solvent catalyst and concentration on the gelation and porosity of hexylene-bridged polysilsesquioxanes. J Non Cryst Solids 362:82–94
49. Brinker CJ, Scherer GW (1990) Sol–gel science: the physics and chemistry of sol–gel processing. Academic Press, San Diego, pp 373–384
50. Yokogawa H, Yokoyama M (1995) Hydrophobic silica aerogels. J Non Cryst Solids 186:23–29
51. Shewale PM, Rao AV, Rao AP (2008) Effect of different trimethyl silylating agents on the hydrophobic and physical properties of silica aerogels. Appl Surf Sci 254:6902–6907
52. Orgaz F, Rawson H (1986) Characterization of various stages of the sol–gel process. J Non Cryst Solids 82:57–68
53. Ogata M, Kinjo N, Kawata T (1993) Effects of crosslinking on physical properties of phenol-formaldehyde Novolac cured epoxy resins. J Appl Polym Sci 48:583–601
54. Kjøniksen AL, Nyström B (1996) Effects of polymer concentration and cross-linking density on rheology of chemically cross-linked poly(vinyl alcohol) near the gelation threshold. Macromolecules 29:5215–5222
55. Xiong L, Hu X, Liu X, Tong Z (2008) Network chain density and relaxation of in situ synthesized polyacrylamide/hectorite clay nanocomposite hydrogels with ultrahigh tensibility. Polymer 49:5064–5071
56. Soleimani Dorcheh A, Abbasi MH (2008) Silica aerogel; synthesis properties and characterization. J Mater Process Technol 199:10–26
57. Kanamori K (2011) Organic–inorganic hybrid aerogels with high mechanical properties via organotrialkoxysilane-derived sol–gel process. J Ceram Soc Jpn 119:16–22
58. Thorne-Banda H, Miller T (2011) In: Aegerter MA, Leventis N, Koebel MM (eds) Aerogels handbook. Springer, New York
59. Prakash SS, Brinker CJ, Hurd AJ, Rao SM (1995) Silica aerogel films prepared at ambient pressure by using surface derivatization to induce reversible drying shrinkage. Nature 374:439–443
60. Scherer GW (1992) Stress development during supercritical drying. J Non Cryst Solids 145:33–40